

# Peculiar structures in the infrared spectra of new iron selenide $K_{0.83}Fe_{1.53}Se_2$ : implication for the electronic structure

Z. G. Chen, R. H. Yuan, T. Dong, G. Xu, Y. G. Shi, P. Zheng, J. L. Luo, J. G. Guo, X. L. Chen, and N. L. Wang  
*Beijing National Laboratory for Condensed Matter Physics,  
Institute of Physics, Chinese Academy of Sciences, Beijing 100190, China*

We report an infrared spectroscopy study on  $K_{0.83}Fe_{1.53}Se_2$ , a semiconducting parent compound of the new iron-selenide system. The major spectral features are found to be distinctly different from all other Fe-based superconducting systems. Our measurement revealed two peculiar spectral structures: a double peak structure between 4000-6000  $cm^{-1}$  and abundant phonon modes much more than those expected for a 122 structure. We elaborate that those features could be naturally explained from the blocked antiferromagnetism due to the presence of Fe vacancy ordering as determined by recent neutron diffraction experiments. The double peaks reflect the coexistence of ferromagnetic and antiferromagnetic couplings between the neighboring Fe sites.

PACS numbers: 74.70.Xa, 74.25.Gz, 74.25.nd

After three years intensive studies on the Fe-based superconductors, much progress has been made in understanding the properties and principles of materials. Similar to the high- $T_c$  cuprates, the superconductivity in Fe-based compounds is found to be in close proximity to an antiferromagnetic (AFM) order<sup>1,2</sup>. Superconductivity emerges when the magnetic order was suppressed by electron or hole doping or application of pressure<sup>1-5</sup>. Although the phase diagram of Fe-pnictides appears very similar to that of high- $T_c$  cuprates, distinct differences exist between them. The undoped compounds in cuprates are Mott insulators, by contrast, the parent compounds in Fe-pnictides are spin-density-wave (SDW) metals. Electronic structure studies show that the Fermi surfaces and band structures of Fe-based compounds are qualitatively similar. In particular, all the compounds show small compensating hole and electron Fermi surfaces locating respectively near the Brillouin zone center and corner<sup>6</sup>. It is widely believed that the inter-pocket scattering between the electron and hole pockets is crucial to the superconducting pairing<sup>7-12</sup>.

However, the recent discovery of superconductivity over 30 K in  $K_xFe_2Se_2$ <sup>13</sup> poses a strong challenge to the above picture. Soon after this discovery, a resistivity study on a related system  $(Tl,K)Fe_{2-x}Se_2$  indicated that the superconducting phase evolves from an insulating phase rather than an SDW metal<sup>14</sup>. Subsequent angle resolved photoemission spectroscopy (ARPES) studies revealed that the Fermi surface (FS) topologies of those compounds are very different from previously known materials. Only the electron pockets are present in the superconducting compounds, while the hole bands sink below the Fermi level, indicating that the inter-pocket scattering between the hole and electron pockets is not an essential ingredient for superconductivity<sup>15,16</sup>. More surprisingly, recent muon-spin relaxation ( $\mu$ SR)<sup>17,18</sup>, neutron diffraction<sup>19-21</sup>, resistivity and magnetization<sup>22</sup> measurements on  $A_xFe_{2-y}Se_2$  ( $A=K, Rb, Cs, Tl$ ) revealed a coexistence of superconductivity with a strong AFM order. In particular, the neutron experiments

revealed a completely new type of magnetic order, a blocked checkerboard antiferromagnetism for the system. The ordered magnetic moment  $\sim 3.31 \mu_B/Fe$  is unprecedentedly large, and the magnetic transition occurs at a record high temperature of  $T_N=559$  K below the formation of an Fe vacancy ordering with a  $\sqrt{5} \times \sqrt{5} \times 1$  superlattice pattern at  $T_S \sim 578$  K.

Infrared spectroscopy is a powerful technique to investigate charge dynamics and band structure of a material as it probes both free carriers and interband excitations. In this paper, we report an infrared spectroscopy study on the insulating parent compound of  $K_{0.83}Fe_{1.53}Se_2$ . Our measurement revealed a small energy gap in the low-lying excitation. Furthermore, a double peak structure between 4000-6000  $cm^{-1}$  and abundant phonon lines much more than those expected for a standard 122 structure were observed. Those peculiar features were not seen in any other Fe-pnictides/chalcogenides, and could be taken as the characteristic optical spectral structures for this system. We elaborate that those features could be naturally explained from the blocked antiferromagnetism due to the presence of Fe vacancy ordering as determined by recent neutron diffraction experiments. Those measurement results are important in understanding the new Fe-selenide system.

The single crystal samples were grown from self-melting method with a nominal starting composition of  $K:Fe:Se=1:2:2$ . FeSe was firstly synthesized by reacting Fe powder and Se powder at 700<sup>o</sup>C for 15 hours twice. K pieces and FeSe powder were then put into an alumina crucible and sealed in a Ta tube with Argon gas at the pressure of 1 atom. The Ta tube was further sealed into a quartz tube in vacuum. The crystal growth was taken place in a box furnace. The crucible was slowly heated up to 1027<sup>o</sup>C and held for 5 hours, then cooled down to 750<sup>o</sup>C at a rate of 5<sup>o</sup>C/hour. Plate-like single crystals with shiny surface were obtained after breaking the crucible.

The crystals were characterized by X-ray diffraction (XRD), scanning electron microscopy equipped with the

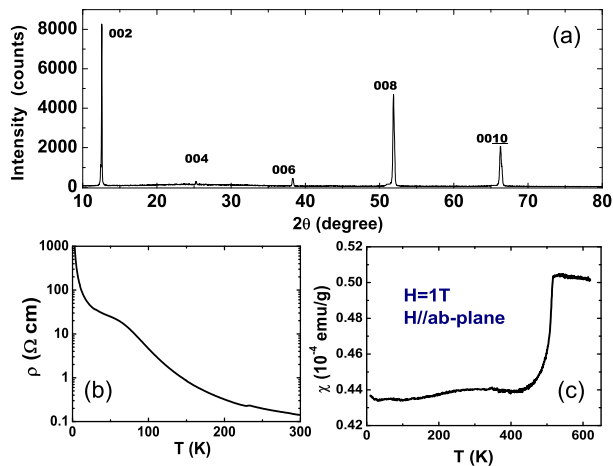


FIG. 1: (Color online) (a) The x-ray-diffraction pattern of the crystal. Only  $(00l)$  diffraction peaks are observed. (b) The ab-plane resistivity curves versus temperature. (c) The magnetic susceptibility curve versus temperature. The sharp drop near 519 K indicates the development of the antiferromagnetic order.

energy dispersive X-ray (EDX) spectroscopy, dc resistivity, and magnetic susceptibility measurements. Figure 1 (a) shows the XRD pattern for the single crystal with Cu  $K\alpha$  radiation. As expected, only  $(00l)$  diffraction peaks are observed, indicating that the crystallographic  $c$  axis is perpendicular to the cleaved surface. The  $c$ -axis lattice constant is determined to be 14.10 Å. The average composition determined by the EDX analysis on several different positions of the crystal is found to be close to  $K_{0.83}Fe_{1.53}Se_2$ . We use this composition throughout the paper. However, we remark that this composition formula should be considered only as an approximate one since the accuracy of EDX analysis is not very high. Figure 1 (b) shows the in-plane dc resistivity data measured by four-leads method in a Quantum Design physical properties measurement system (PPMS). It shows an insulating behavior. The resistivity increases by several orders with decreasing temperature from 300 K. Figure 1 (c) shows the magnetic susceptibility data below 620 K measured also in PPMS under the field of 1 Tesla. The sample shows a very sharp magnetic transition at 518 K. Clearly, the crystal is an AFM insulator.

Optical measurement was done on a Bruker Vertex 80v spectrometer in the frequency range from 40 to 25000  $cm^{-1}$ . The crystal surface was found to be relatively stable, being comparable to other Fe-pnictides/chalcogenides. The sample was mounted on an optically black cone locating at the cold finger of the cryostat. Freshly cleaved surface was obtained just before pumping the cryostat. An *in-situ* gold and aluminum overcoating technique was used to get the reflectance  $R(\omega)$ . The optical data were found to be highly reproducible. The real part of conductivity  $\sigma_1(\omega)$  is obtained by the Kramers-Kronig transformation of  $R(\omega)$ . Figure 2 shows the  $R(\omega)$  and  $\sigma_1(\omega)$  spectra for the sample over

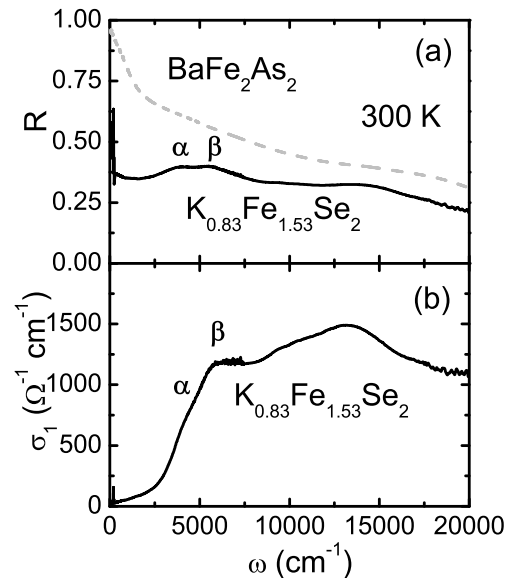


FIG. 2: The optical reflectance  $R(\omega)$  (a) and conductivity  $\sigma_1(\omega)$  (b) at room temperature up to 20000  $cm^{-1}$ .  $\alpha$  and  $\beta$  indicate two-peaks interband transition structure. The reflectance curve of  $BaFe_2As_2$  at 300 K was added for a comparison<sup>23</sup>.

broad frequencies up to 20000  $cm^{-1}$ . The overall reflectance is rather low, roughly close to the value of 0.4. This behavior is different from all other Fe-pnictide compound as well as FeTe. As a comparison, we also plot the in-plane reflectance of a  $BaFe_2As_2$  crystal<sup>23</sup> in Fig. 2 (a) which is considerably higher. The  $\sigma_1(\omega)$  shows vanishing conductivity at low frequency, indicating insulating-like response. Detailed spectral features at low frequency will be presented below. Strong interband transition peaks were seen near 5000  $cm^{-1}$  and 13000  $cm^{-1}$ . Actually the reflectance spectrum displays two peaks (labelled as  $\alpha$  and  $\beta$ ) for the interband transitions at lower energy scale, roughly at  $\sim 4500$   $cm^{-1}$  (0.56 eV) and 6000  $cm^{-1}$  (0.75 eV). Relatively weak features are seen in the  $\sigma_1(\omega)$  spectrum.

Figure 3 shows the temperature dependence of the optical spectra at lower energy scales. The left panels (3 (a) and (c)) show the  $R(\omega)$  and  $\sigma_1(\omega)$  spectra up to 8000  $cm^{-1}$ , the right panels (3 (b) and (d)) show the spectra in the expanded low frequency region within 400  $cm^{-1}$ . Because the spectra display a weak temperature dependence, we show the spectra only at three different temperatures. The almost constant value of  $R(\omega)$  down to very low frequency yields evidence for a non-metallic infrared response. The further decrease of the low frequency  $R(\omega)$  at lower temperature provides additional support for the semiconducting or insulating behavior. Correspondingly, there is no free carrier Drude response at low frequency in the conductivity spectra (Fig. 3 (c) and (d)). The slight enhancement of the low- $\omega$  optical conductivity at higher temperature can be attributed to the thermally-activated hopping of electrons.

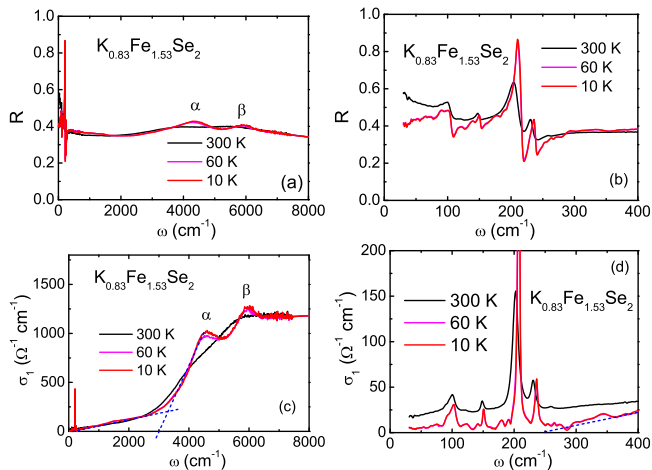


FIG. 3: (Color online) (a) optical reflectance  $R(\omega)$  spectra at different temperatures up to  $8000 \text{ cm}^{-1}$ . (b) An expanded plot of  $R(\omega)$  spectra below  $400 \text{ cm}^{-1}$ . (c) the conductivity  $\sigma_1(\omega)$  spectra of the sample at different temperatures up to  $8000 \text{ cm}^{-1}$ . (d) An expanded plot of  $\sigma_1(\omega)$  spectra below  $400 \text{ cm}^{-1}$ . The dashed straight lines are used for extrapolation of energy gaps.

Besides the semiconducting/insulating response, there exist two prominent features in the spectra. First, the two-peaks interband transition structure in the mid- to near infrared region between  $\sim 4500 \text{ cm}^{-1}$  and  $6000 \text{ cm}^{-1}$  seen at room temperature become very prominent at low temperature, as shown clearly in Fig. 3 (a) and (c). Second, as evidenced clearly in Fig. 2 (b) and (d), there exist over 10 phonon peaks at the low frequencies. It should be noted, for the standard 122 structure, only two infrared active phonon modes should be present in the ab-plane infrared spectra<sup>24</sup>.

As the superconductivity is in close proximity to the insulating phase, it is extremely important to identify the properties and nature of this insulating compound. A crucial question is whether the compound is a Mott insulator or a band insulator? This would be a starting point for understanding the material. Actually, there have been controversial points of views on the basis of weak-coupling or strong coupling approaches in understanding the magnetism and superconductivity in Fe-pnictides/chalcogenides ever since the discovery of Fe-based superconductors.

From Fig. 3 (c) and (d), we could see that the low- $\omega$   $\sigma_1(\omega)$  at 10 K is dominated by the phonon peaks with a vanishing electronic contribution roughly below  $250 \text{ cm}^{-1}$ . Above this energy the conductivity increases almost linearly up to  $3000 \text{ cm}^{-1}$  at which much stronger interband transitions appear. Based on this direct observation, we can assign the sharp increase near  $3000 \text{ cm}^{-1}$  ( $\sim 0.37 \text{ eV}$ ) in  $\sigma_1(\omega)$  as a gap arising from a direct interband transition. However, below  $3000 \text{ cm}^{-1}$ , there still exist sizeable absorptions, most likely from an indirect interband transitions assisted by the impurities and collective boson excitations. But this absorption en-

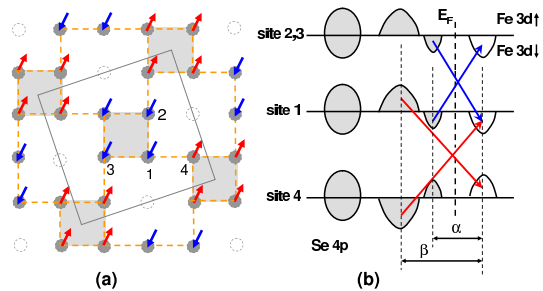


FIG. 4: (Color online) (a) The magnetic structure determined by the neutron diffraction experiment<sup>19</sup>. The grey solid lines represent a  $\sqrt{5} \times \sqrt{5} \times 1$  unit cell. (b) A schematic picture for the band occupation for each Fe site. Site 4 has opposite spin-polarized occupations with site 1, 2, and 3. Possible d-d transitions are indicated by the arrows. The double peaks represents the coexistence of the ferro- and antiferromagnetic correlations between the neighboring sites.

ergy scale is much smaller,  $\sim 250 \text{ cm}^{-1}$  ( $30 \text{ meV}$ ) as obtained from a linear extrapolation of the  $\sigma_1(\omega)$  below  $3000 \text{ cm}^{-1}$ . Since the gap (even for the direct energy gap) is small, the compound is not likely to be a Mott insulator, given the fact that the Mott gap should have an energy scale comparable to the on-site Coulomb repulsion energy  $U$ . The indirect nature of the interband transition for the lowest gap in the electronic excitations appears also to rule out the possibility of the presence of a charge transfer energy gap as a case established for the case of high- $T_c$  cuprates. We suggest that the compound should be considered as a small band gap semiconductor. Recent band structural calculations<sup>25,26</sup> could indeed reproduce the semiconducting band structures by taking account of the ordering of Fe vacancies with the experimentally determined blocked checkerboard AFM order although the calculated band gaps are larger,  $\sim 0.4\text{-}0.6 \text{ eV}$ . It is also in agreement with recent ARPES measurement<sup>16</sup> on a superconducting sample where the band renormalization factor is found to be only 2.5.

As mentioned above, the double interband transition peaks in the mid- to near-infrared region and abundant phonon modes below  $400 \text{ cm}^{-1}$  are two other interesting observations. They were not seen in any other Fe-pnictides/chalcogenides, and therefore, could be taken as the characteristic optical spectral features for this specific system. We believe that both should be strongly associated with the Fe vacancy ordering in the compound. We shall first address the origin of the double peak structure. For the investigated system  $A_x\text{Fe}_{2-y}\text{Se}_2$ , Fe vacancies obviously exist. Those Fe vacancies should form ordered pattern otherwise it is difficult to imagine that superconductivity could emerge in this system. For the composition of  $\text{Fe} \sim 1.5$ , one expects to see one vacancy per four Fe sites. Several different Fe vacancy ordering patterns matching with one vacancy per four sites have been proposed<sup>14,27,28</sup>, they all lead to inequivalent Fe sites in the structure with different coordinated Fe neighbors. This may cause energy difference between bonding

and antibonding states of Fe 3d orbitals, which may explain the observed double peaks structure. However, this possibility is essentially ruled out by the neutron diffraction experiments<sup>19–21</sup>, which indicated a complete absence of an ordering pattern with one vacancy per four Fe sites. Instead, for all available  $A_x\text{Fe}_{2-y}\text{Se}_2$  ( $A=\text{K, Rb, Cs, Tl}$ ) samples with different Fe compositions, neutron measurements<sup>21</sup> revealed a Fe vacancy ordering with a  $\sqrt{5} \times \sqrt{5} \times 1$  superlattice pattern below room temperature. In this ordering pattern, all occupied Fe sites are equivalent. The major difference for different Fe compositions would be a change of occupation rates for both occupied and vacant Fe sites.

We find that the  $\alpha$  and  $\beta$  double peaks could be naturally explained by the peculiar magnetic structure (shown in Fig. 4 (a)) determined by the neutron diffraction experiment<sup>19–21</sup>. In this ordering pattern, each Fe site is ferromagnetic coupled with two neighboring Fe sites and antiferromagnetic coupled with the third neighboring Fe site. To simplify our discussions, we consider that the Fe ion has a 2+ valance state with  $3d^6$  configuration. We ignore possible itinerant d electrons from certain orbitals, and assume that the Hund's rule coupling energy is larger than the crystal field splitting energy, then the 5 electrons would fully occupy 5 orbitals in a spin polarized direction, the other one electron would occupy one of the orbital in the opposite spin direction, leaving the other four orbitals completely unoccupied. The band occupation for each Fe site is schematically shown in Fig. 4 (b). In Fig. 4 (a), the Fe 1, Fe2, and Fe3 have the same spin-polarized occupations, the Fe 4 has the opposite spin-polarized occupations. Because the optical transitions do not involve spin-flip process, the possible d-d transitions (via hybridization with Se 4p orbitals) are indicated by the arrows, representing the transitions from the occupied states at one Fe site to the unoccupied states at nearest-neighboring Fe sites. From this

schematic diagram, we can see that the  $\alpha$  peak comes from the transitions between the neighboring ferromagnetic ordered sites and the  $\beta$  transition from the neighboring antiferromagnetic ordered sites. The double peaks represents the coexistence of the ferro- and antiferromagnetic correlations between the neighboring sites.

Another striking feature is the presence of more than 10 phonon peaks at the low frequencies. As we also mentioned, for the standard 122 structure, only two infrared active phonon modes should be present in the ab-plane infrared spectra<sup>24</sup>. As the neutron measurements indicate the formation of  $\sqrt{5} \times \sqrt{5} \times 1$  superlattice pattern due to the Fe vacancy ordering, the crystallographic unit cell is actually enlarged as  $\text{K}_2\text{Fe}_4\text{Se}_5$ .<sup>19</sup> The composition  $\text{K}_{0.83}\text{Fe}_{1.53}\text{Se}_2$  deviates from this perfect 245 compound, leading to a modified occupation rates in the occupied and vacant Fe sites (or disorders) based on the neutron diffraction measurements. Then more phonon modes than the tetragonal  $\text{ThCr}_2\text{Si}_2$  structure would be allowed in optical measurement.

To conclude, we performed infrared spectroscopy study on semiconducting of  $\text{K}_{0.83}\text{Fe}_{1.53}\text{Se}_2$ . We identify that the compound is a small energy gap semiconductor. Our infrared measurement also revealed two other characteristic spectral features which are specific to the materials but absent in other Fe-pnictides/chalcogenides: a double peak structure near  $4000\text{-}6000\text{ cm}^{-1}$  and abundant phonon modes much more than those expected for a standard 122 structure. We elaborated that both could be naturally explained from the peculiar blocked AFM structure due to the presence of Fe vacancy ordering.

We acknowledge helpful discussions with Z. Fang, D. Xi, G. M. Zhang, H. Ding, Z. Y. Lu, T. Xiang, M. F. Fang, G. F. Chen, Q. Si and Y. P. Wang. This work was supported by the NSFC, CAS and the 973 project of the MOST.

- 
- <sup>1</sup> J. Dong, H. J. Zhang, G. Xu, Z. Li, G. Li, W. Z. Hu, D. Wu, G. F. Chen, X. Dai, J. L. Luo, Z. Fang, and N. L. Wang, *Europhys. Lett.* **83**, 27006 (2008).
- <sup>2</sup> Clarina de la Cruz, Q. Huang, J. W. Lynn, Jiying Li, W. Ratcliff II, J. L. Zarestky, H. A. Mook, G. F. Chen, J. L. Luo, N. L. Wang, and Pengcheng Dai, *Nature* **453**, 899 (2008).
- <sup>3</sup> G. F. Chen, Z. Li, D. Wu, G. Li, W. Z. Hu, J. Dong, P. Zheng, J. L. Luo, and N. L. Wang, *Phys. Rev. Lett.* **100**, 247002 (2008).
- <sup>4</sup> M. Rotter, M. Tegel, D. Johrendt, *Phys. Rev. Lett.* **101**, 107006 (2008).
- <sup>5</sup> M. S. Torikachvili, *Phys. Rev. Lett.* **101**, 057006 (2008).
- <sup>6</sup> D. J. Singh, *Physica C* **469**, 418 (2009).
- <sup>7</sup> K. Kuroki, S. Onari, R. Arita, H. Usui, Y. Tanaka, H. Kontani, and H. Aoki, *Phys. Rev. Lett.* **101**, 087004 (2008).
- <sup>8</sup> I. I. Mazin, D.J. Singh, M.D. Johannes, and M.H. Du, *Phys. Rev. Lett.* **101**, 057003 (2008).
- <sup>9</sup> A. D. Christianson, A. D. Christianson, M. D. Lumsden, O. Delaire, M. B. Stone, D. L. Abernathy, M. A. McGuire, A. S. Sefat, R. Jin, B. C. Sales, D. Mandrus, E. D. Mun, P. C. Canfield, J. Y. Y. Lin, M. Lucas, M. Kresch, J. B. Keith, B. Fultz, E. A. Goremychkin, and R. J. McQueeney, *Phys. Rev. Lett.* **101**, 157004 (2008).
- <sup>10</sup> P. Richard, T. Sato, K. Nakayama, S. Souma, T. Takahashi, Y.-M. Xu, G. F. Chen, J. L. Luo, N. L. Wang, and H. Ding, *Phys. Rev. Lett.* **102**, 047003 (2009).
- <sup>11</sup> F. Wang, H. Zhai, Y. Ran, A. Vishwanath, and D.-H. Lee, *Phys. Rev. Lett.* **102**, 047005 (2009).
- <sup>12</sup> M. M. Korshunov & I. Eremin, *Phys. Rev. B* **78**, 140509(R) (2008).
- <sup>13</sup> J. Guo, S. Jin, G. Wang, S. Wang, K. Zhu, T. Zhou, M. He and X. Chen, *Phys. Rev. B* **82**, 180520 (2010).
- <sup>14</sup> M. H. Fang, H. Wang, C. Dong, Z. Li, C. Feng, J. Chen, and H.Q. Yuan, *Europhys. Lett.* **94**, 27009 (2011).
- <sup>15</sup> Y. Zhang, L. X. Yang, M. Xu, Z. R. Ye, F. Chen, C. He, J. Jiang, B. P. Xie, J. J. Ying, X. F. Wang, X. H. Chen, J. P. Hu, and D. L. Feng, *Nature Materials* **10**, 273 (2011).

- <sup>16</sup> T. Qian, X.-P. Wang, W.-C. Jin, P. Zhang, P. Richard, G. Xu, X. Dai, Z. Fang, J.-G. Guo, X.-L. Chen, and H. Ding, Phys. Rev. Lett. **106**, 187001 (2011).
- <sup>17</sup> Z. Shermadini, A. Krzton-Maziopa, M. Bendele, R. Khasanov, H. Luetkens, K. Conder, E. Pomjakushina, S. Weyeneth, V. Pomjakushin, O. Bossen, and A. Amato, Phys. Rev. Lett. **106**, 117602 (2011).
- <sup>18</sup> V. Yu. Pomjakushin, D. V. Sheptyakov, E. V. Pomjakushina, A. Krzton-Maziopa, K. Conder, D. Chernyshov, V. Svitlyk, and Z. Shermadini, Phys. Rev. B **83**, 144410 (2011).
- <sup>19</sup> Wei Bao, Q. Huang, G. F. Chen, M. A. Green, D. M. Wang, J. B. He, X. Q. Wang, and Y. Qiu, arXiv:1102.0830.
- <sup>20</sup> F. Ye, S. Chi, Wei Bao, X. F. Wang, J. J. Ying, X. H. Chen, H. D. Wang, C. H. Dong, and Minghu Fang, arXiv:1102.2882.
- <sup>21</sup> Wei Bao, G. N. Li, Q. Huang, G. F. Chen, J. B. He, M. A. Green, Y. Qiu, M. Wang, and J. L. Luo, arXiv:1102.3674.
- <sup>22</sup> R. H. Liu, X. G. Luo, M. Zhang, A. F. Wang, J. J. Ying, X. F. Wang, Y. J. Yan, Z. J. Xiang, P. Cheng, G. J. Ye, Z. Y. Li, and X. H. Chen, Europhys. Lett. **94**, 27008 (2011).
- <sup>23</sup> W. Z. Hu, J. Dong, G. Li, Z. Li, P. Zheng, G. F. Chen, J. L. Luo, and N. L. Wang, Phys. Rev. Lett. **101**, 257005 (2008).
- <sup>24</sup> A. Akrap, J. J. Tu, L. J. Li, G. H. Cao, Z. A. Xu, and C. C. Homes, Phys. Rev. B **80**, 180502(R) (2009).
- <sup>25</sup> C. Cao and J. Dai, arXiv:1102.1344.
- <sup>26</sup> X.-W. Yan, M. Gao, Z.-Y. LU, and T. Xiang, arXiv:1102.2215.
- <sup>27</sup> X.-W. Yan, M. Gao, Z.-Y. LU, and T. Xiang, Phys. Rev. Lett. **106**, 087005 (2011).
- <sup>28</sup> Rong Yu, Jian-Xin Zhu, and Qimiao Si, Phys. Rev. Lett. **106**, 186401 (2011).